Science Advances
AAAS

advances.sciencemag.org/cgi/content/full/6/47/eabb5643/DC1

Supplementary Materials for

Ion-molecule interactions enable unexpected phase transitions in organic-inorganic aerosol

David S. Richards, Kristin L. Trobaugh, Josefina Hajek-Herrera, Chelsea L. Price, Craig S. Sheldon, James F. Davies, Ryan D. Davis*

*Corresponding author. Email: rdavis5@trinity.edu

Published 18 November 2020, *Sci. Adv.* **6**, eabb5643 (2020)
DOI: 10.1126/sciadv.abb5643

This PDF file includes:

Supporting Text

Relating Shape Relaxations to Phase.

Upon merging of two droplets, the shape of the merged dimer deviates significantly from that of a perfect sphere. Over time, for liquid droplets, merged dimers relax to a spherical shape to minimize surface energy. The time it takes to relax to sphericity is related to the viscosity (η), surface tension (σ), density, and radius (r) of the relaxed sphere (*14-18*). Above viscosities of ~40 mPa s, such as is the case in the present study, merged droplets are in the overdamped regime and relaxation occurs gradually with no oscillations in shape (*14,17*). Thus, in the overdamped regime, the characteristic timescale of coalescence (τ) of a liquid can be related to viscosity through Equation S1:

$$\tau \approx \frac{\eta r}{\sigma} \qquad \text{(S1)}$$

In the present study, timescales (τ or observation time, t_{obs}) were used to differentiate between RH-dependent phase behavior of viscous liquids and gelatinous (semi-)solid. For viscous liquids, thickening can occur gradually over a wide RH range (*13-19*), and gelation can undergo an abrupt phase transition (*13,14,29*), as described extensively in our previous publication (*14*). Because the focus was to probe an abrupt phase transformation, in addition to exploring trends in aerosol viscosity, we used a fixed equilibration time of 5 min for all experiments prior to merging droplets (analogous to the approach of using fixed residence times used when probing ice nucleation or efflorescence). This approach, with a limited residence time, has been demonstrated to be effective at identifying gel transitions and inferring RH-dependent trends in viscosity (*14*). (At longer equilibration timescales, inferred viscosity can increase by ~1 order of magnitude (*14*), which is a common uncertainty when inferring viscosity across many orders of magnitude (*17*), and the RH-dependent trends remain similar to a 5 min equilibration timescale (*14*).) Unlike liquids, rigid gels (and solids, in general) do not show any coalescence upon merging (at least within practical timescales), providing a way to distinguish between different phases.

Gels are frequently described as non-Newtonian, i.e., they can have different viscoelastic properties depending on the shear stress applied (*14*). When shear stress is low or non-existent, as is the case in the present study, gels may behave like solids below the gelation limit. Thus it is not expected that gels would necessarily flow together, even at long timescales (i.e., t_{obs}), consistent with our observations. For atmospheric aerosol particles, the practical implications of non-Newtonian fluid behavior may manifest as non-uniform diffusion throughout the particle (*44*), and thus potential non-uniform hygroscopicity and oxidative aging. (Note, for shear-thickening gels, the opposite may be true, where it is possible to have a gel system that behaves mechanically like a solid when shear is high, but behave like a liquid under low shear.) Despite the increased water content associated with $CaCl_2$, the semi-solid $CaCl_2$-organic network apparently maintains the rigidity of the droplets. Due to the semi-solid properties of the observed gels, it may not be appropriate to describe the gels as having a single dynamic viscosity, and thus data is discussed in terms of timescales as well as viscosity (because it is evident from the coalescence measurements, where coalescence could be captured by a single-exponential relaxation to sphericity, that the Ca-organic droplets are Newtonian fluids that have a single dynamic viscosity prior to RH_{gel}). A phase transition is then identified by the abrupt change in timescale (and inferred viscosity) that occurs over a narrow RH range.

Further Evidence for a Gel Phase Transition

RH-dependent trends in phase: Crystalline solids, glasses, and semi-solid gels would all exhibit rigidity over long timescales, as observed with the rigid, divalent inorganic-organic droplets. No efflorescence transition is observed (i.e., no crystal growth and loss of particle-phase water), as demonstrated in Fig. S4B. Thus, we conclude that the observed rigid droplets are not crystalline solids nor are they partially crystalline, as confirmed with far-field images (Fig. S4B). To further assess whether our observations are consistent with that of gel or glass formation, we compared the phase behavior of ternary

Ca^{2+}-organic droplets to that of $MgSO_4$ (known to form a gel network at ~30-50% RH) (*13,14*) and sucrose (with a glass transition at ~23% RH) (*17*). $MgSO_4$ was chosen as the gel analogue for comparison to our observations because $MgSO_4$ gels have been well-studied and are known to form in a comparable RH range as the rigid Ca^{2+}-organic structures (*13,14*). Sucrose was chosen to be representative of the behavior of a glass-forming saccharide because the lower-limit of τ is at a similar RH as that of 1:1 Ca^{2+}:gluconic acid (~55% RH). For the size of droplets used in this study, it would take ~20 years for complete coalescence of two glassy particles. Thus, we are unable to probe the glass transition directly. However, for comparison to our observations with Ca^{2+}-organic microdroplets, we are able to explore trends in the phase behavior of glass-forming saccharides as the glass transition is approached

Fig. S5A shows the timescales associated with merging events for $MgSO_4$ and sucrose, and compares these to 1:1 Ca^{2+}:gluconic acid. Over the range of RH values studied, the overall trend for binary sucrose is a gradual increase in viscosity, with an order of magnitude increase in τ for every 5-7% decrease in RH, similar to the trends observed with the binary organics and consistent with previous reports (*13-19*). This gradual increase in timescale for binary sucrose differs from the RH-dependent rheological behavior we observe for the Ca^{2+}-organic droplets, which exhibited a much steeper transition to rigid structures.

In contrast to the gradual increase observed with sucrose, the RH-dependent trend for $MgSO_4$ is nearly identical to that of the Ca^{2+}-organic microdroplets, as seen in Fig. S5A comparing $MgSO_4$ to 1:1 Ca^{2+}:gluconic acid droplets. Specifically, merged $MgSO_4$ droplets exhibit a sharp increase in timescale over a narrow range of RH (<5% RH), similar to observations of ternary Ca^{2+}-organic microdroplets. In the case of $MgSO_4$, there is an initial increase in viscosity coincident with the RH at which contact-ion pairing is reported to occur (~35 to 40% RH) (*24*). At ~30% RH, $MgSO_4$ droplets remain completely rigid, consistent with the RH-dependent threshold at which an extensive cross-linked network forms. The behavior of $MgSO_4$ micro-gels is nearly identical to the Ca-organic droplets, validating the identification of Ca-organic droplets as existing as gels below a threshold RH.

Water content of the rigid droplets: As additional confirmation of a gel transition and to further rule out a humidity-induced glass transition, we used Raman spectroscopy to qualitatively compare the water content in ternary $CaCl_2$:gluconic acid droplets to that of binary droplets. RH-induced glass transitions occur as water content decreases with decreasing RH (*17*). However, as shown in Fig. S5B, ternary $CaCl_2$-gluconic acid droplets have increased water content relative to binary gluconic acid droplets (by weight fraction). Increased water content is indeed expected due to the hygroscopicity of $CaCl_2$ and predicted from aerosol thermodynamic models (AIOMFAC (*29*); see Table S1). Thus, an RH-dependent glass transition does not explain the formation of rigid structures with ternary $CaCl_2$ droplets. Rather, the rigid structure and elevated water content of Ca-organic droplets demonstrate an RH-dependent (hydro-)gel transition.

Expectations from Mixing Approximations.

Although it is well established that mixtures of multiple fluids will have different properties than the individual components (*15,16*), predictions from simple viscosity mixing rules for ternary aqueous mixtures do not predict the observed behavior with divalent inorganics/organic mixtures. Rather, mixing rules such as the Bosse ideal mixing rule and the mixing of binary water-activity dependent viscosities predict that for a mixture of multiple components, the viscosity of the mixture will generally have an intermediate value between that of the two individual components (*15*). Binary NaCl and $CaCl_2$ are hygroscopic and non-viscous relative to binary organics. Thus, the expectation from simple mixing rules is that ternary salt-organics mixtures would have a higher viscosity than the binary salts, but a lower viscosity than the binary organics due to the plasticizing effect of the increased water content (*15,16*). As seen in Fig. S2, it is generally true that ternary NaCl:organic droplets have lower viscosities than the binary organic. The exception is with the carboxylic acids gluconic and glucuronic acid, in which there is a slight increase in timescale (and thus viscosity), likely due to the interaction expected between Na^+ and

the carboxylate groups, where a single Na^+ largely interacts with a single COO^- (*28*), and thus there is limited potential for long-range networks, at least in 1:1 mole ratios. However, even with the carboxylic acids, the influence of Na^+ was small (~1 order of magnitude typical) relative to the effect with $CaCl_2$, and no ternary NaCl-organic mixtures exhibited signs of a phase transformation within the RH range studied (although NaCl may be promoting a glass transition at even lower RH in the carboxylic acid systems). Although the deviation from predicted behavior is subtle for the NaCl-carboxylic acid mixtures, the deviation is extremely pronounced with $CaCl_2$-organic mixtures, even for the neutral molecules, demonstrating that water has no plasticizing effect in these mixtures (indeed, the opposite effect occurs).

Deviations from simple mixing rules with highly oxygenated organics and ions is not entirely unexpected. As noted by Rovelli et al. (*15*), the interactions between ions and oxygenated organics is likely to be complex and non-ideal, particularly under the highly-concentrated conditions representative of atmospheric aerosols. This point is demonstrated very clearly with the $CaCl_2$-organic mixtures studied here, in which a long-range gelatinous network assembles under highly-concentrated conditions not readily accessible in bulk conditions. Thus, for complex mixtures, particularly those containing divalent ions, considering ion-ion and ion-organic interactions is likely essential for accurately representing viscosity and micro-structural properties of atmospheric aerosols.

If we consider the $CaCl_2$-sorbitol system, one of the systems involving a neutral monosaccharide, simple mixing rules under-predict the viscosity by multiple orders of magnitude. $CaCl_2$ is highly hygroscopic and has relatively low viscosity even at high concentrations (*32*) and sorbitol's relatively low viscosity at room temperature and hygroscopicity make it a known plasticizer in food industries. At ~20% RH (below the approximate gelation RH of sorbitol-$CaCl_2$ droplets) aqueous binary $CaCl_2$ is non-viscous, with a viscosity of <1 Pa·s, as inferred from our observations, bulk predictions (*32*), and measurements from other aqueous salts such as $NaNO_3$ (*15*). Sorbitol is also relatively non-viscous at 20% RH, with an estimated viscosity of ~10^4 Pa·s (*14*). If a simple, water-activity based approach (*15*) is used to estimate the viscosity of this mixture (an approach that has been shown to be a good approximation for ternary $NaNO_3$-sucrose mixtures) then the predicted viscosity for a ternary $CaCl_2$-sorbitol mixture would be intermediate between the viscosity of the binary $CaCl_2$ (<1 Pa·s) and binary sorbitol (10^4 Pa·s), e.g., ~30 Pa·s for a ternary $CaCl_2$-sorbitol droplet. However, at a minimum (if t_{obs} is used in place of τ in Eq S1) ternary droplets have a viscosity of 10^8 Pa·s, with an upper-limit of >10^{12} Pa·s (if the largest value for τ from Fig. S3 is used). The viscosity estimate from a simple mixing approach thus under-predicts viscosity by six orders of magnitude or more. Mixing approximations have been developed for and shown to be effective for fluids that do not strongly interact. Understanding and predicting the supramolecular interactions presented here will likely require a different modeling approach to accurately predict, e.g., viscosity and diffusion constants prior to and after assembly of a gel network.

Estimating the Impact of Supramolecular Effects on Diffusion Constants

Ultimately, the goal of many aerosol viscosity predictions is to inform rates of diffusion through the Stokes-Einstein relationship, given in Equation S2

$$\eta = \frac{k_B T}{6\pi D r_d} \quad \text{(S2)}$$

Where k_B is the Boltzmann constant, η is dynamic viscosity, T is temperature, r_d is radius of the diffusing species with diffusion constant D (*6*). For a dynamic viscosity of ~30 Pa·s, as would be predicted from bulk mixing approximations for the ternary sorbitol-$CaCl_2$ system if ion-molecule interactions were not considered (see above), this corresponds to a diffusion constant of ~10^{-13} m^2s^{-1} for a diffusing species if gelation is not considered. Davies et al. (*13*) has demonstrated that the Stokes-Einstein relationship does not accurately predict diffusion constants of water (D_w) in aerosol gels and reported that for $MgSO_4$ gels, diffusion constants are ~10^{-17} m^2s^{-1} at RH below the gel transition (*13*). Thus, application of the Stokes-Einstein equation to bulk mixing approximations of viscosity (i.e., not accounting for ion-molecule

interactions between sorbitol and $CaCl_2$) may over-predict diffusion constants by ~4 orders of magnitude in this system, assuming that diffusion constants in the sorbitol-$CaCl_2$ gels are similar to that in $MgSO_4$ (i.e., 10^{-17} m^2s^{-1} in a gel compared to 10^{-13} m^2s^{-1} assuming a liquid state with bulk approximations). Similarly, not accounting for gelation of the other organics could lead to over predictions of diffusion constants by 4 orders of magnitude or more, with common D_w values of ~10^{-12} to 10^{-13} m^2s^{-1} in small oxygenated organics at 40 to 50% RH (*18*) whereas the organic-inorganic gels are likely to be associated with D_w values of ~10^{-17} m^2s^{-1} as reported for semi-solid aerosol gels (*13*).

More work remains to be done to directly measure diffusion coefficients in these systems, and to establish which theoretical framework is the most accurate for predicting diffusion in systems influenced by supramolecular interactions. However, the estimates made here demonstrate how not accounting for supramolecular interactions in organic-inorganic aerosol may lead to over-predictions by several orders of magnitude or more. Future studies will aim to measure diffusion constants in these systems.

Generalizations and Parameterization

As seen in Fig. 1A of the manuscript, we utilized a range of oxygenated organic molecules with varying structure (linear vs. cyclic), molecular weight, molecular functionality, and O:C in an attempt to constrain the relative factors influencing the supramolecular effects on aerosol phase and RH_{gel}. Gluconic and glucuronic acid (O:C = 1.17), glucose and sorbitol (O:C = 1.0), and N-acetylneuraminic acid (O:C = 0.82) are common atmospheric proxies.

For a first-order approximation of RH_{gel} in ternary mixtures with $CaCl_2$, we conclude that O:C is not an adequate indicator by itself, as shown by the fact that N-acetylneuraminic acid had the highest RH_{gel}, as seen in Fig. 5A, but the lowest O:C. Rather, we focus on molecular functionality. OH groups were common to all systems, but the highest RH_{gel} was observed with the organics that contained both OH groups and a carboxylic acid. To distinguish between the various acids, we considered molecular weight to be the most likely reason behind the differing RH_{gel} considering the established connection between molecular weight and gelation (*22*,*33*) (although we cannot entirely rule out contributions from other functional groups on N-acetylneuraminic acid, such as the acetylamino group). Thus, we have parameterized our data to be predictive of RH_{gel} for 1:1 (by mole) ternary mixtures of $CaCl_2$ and oxygenated organics based on molecular weight and molecular functionality, focusing specifically on the presence of OH and COOH groups, as given by Eq. S3:

$$RH_{gel} = 24(\pm 2) + (0.15(\pm 0.02) \times MW - 6(\pm 4)) \times N_{COOH} \quad \text{(S3)}$$

where MW is the molecular weight of the organic molecule and N_{COOH} is the number of carboxylic acid groups on the molecules. This parameterization is shown here to be valid for N_{COOH} = 0 or 1, MW between 180 and 310 Da, and molecules with O:C between 0.82 and 1.17. The first term is the average RH_{gel} of the neutral organics (sorbitol and glucose) while the latter terms are from an adjusted linear fit to the data for carboxylic acids. In reality, RH_{gel} will not follow a linear trajectory for increasingly higher MW, so further work must be done before establishing a parameterization that is more broadly applicable. However, this parameterization is likely to be useful for a first-order approximation of RH_{gel} for other oxygenated organics, as long as they contain the appropriate functional groups to allow multiple ion binding sites.

From literature observations of Ca-organic interactions in bulk fluids (*37*) we can make some generalizations about molecules that are most likely to exhibit an ion-molecule effect. As suggested for bulk solutions (*37*), for relatively strong Ca^{2+}-organic binding, the ion must have access to two OH groups. Thus, we can generalize that for a supramolecular effect, any oxygenated molecule with two vicinal (or two accessible) OH groups or a carboxylic acid group may experience ion-molecule interactions with divalent ions that can influence physical properties, such as viscosity (in the case of carboxylic acids, even monovalent ions may influence viscosity, as suggested with NaCl-gluconic and –

glucuronic acid mixtures, although the effect is much less pronounced than with divalent ions). For molecules with multiple potential binding sites (for example, two neighboring OH groups and a carboxylic acid) there is the potential for long-range networks to develop. Thus, we posit that for a six-carbon molecule, a minimum of four oxygen atoms would likely be required for a gel transition (O:C of 0.67) whereas a minimum of two vicinal OH groups or one carboxylic acid (O:C of 0.33) would be necessary for ion-molecule-induced thickening (although at an O:C of 0.33, liquid-liquid phase separation is likely (*10*), in which case strong ion-molecule interaction is less likely). A molecule such as 1,2,6-hexanetriol (O:C = 0.5), which does not phase separate from NaCl mixtures (*10*) is an example of a molecule that may have ion-molecule induced thickening without a rigid gel transition (similar to the effect of 10:1 sorbitol:$CaCl_2$) whereas molecules such as 5,6-hydroxyhexanoic acid (O:C = 0.67) and 1,2,5,6-hexanetetrol (O:C = 0.67) have the potential for a gel transition. Future work will focus on testing the validity of these generalizations.

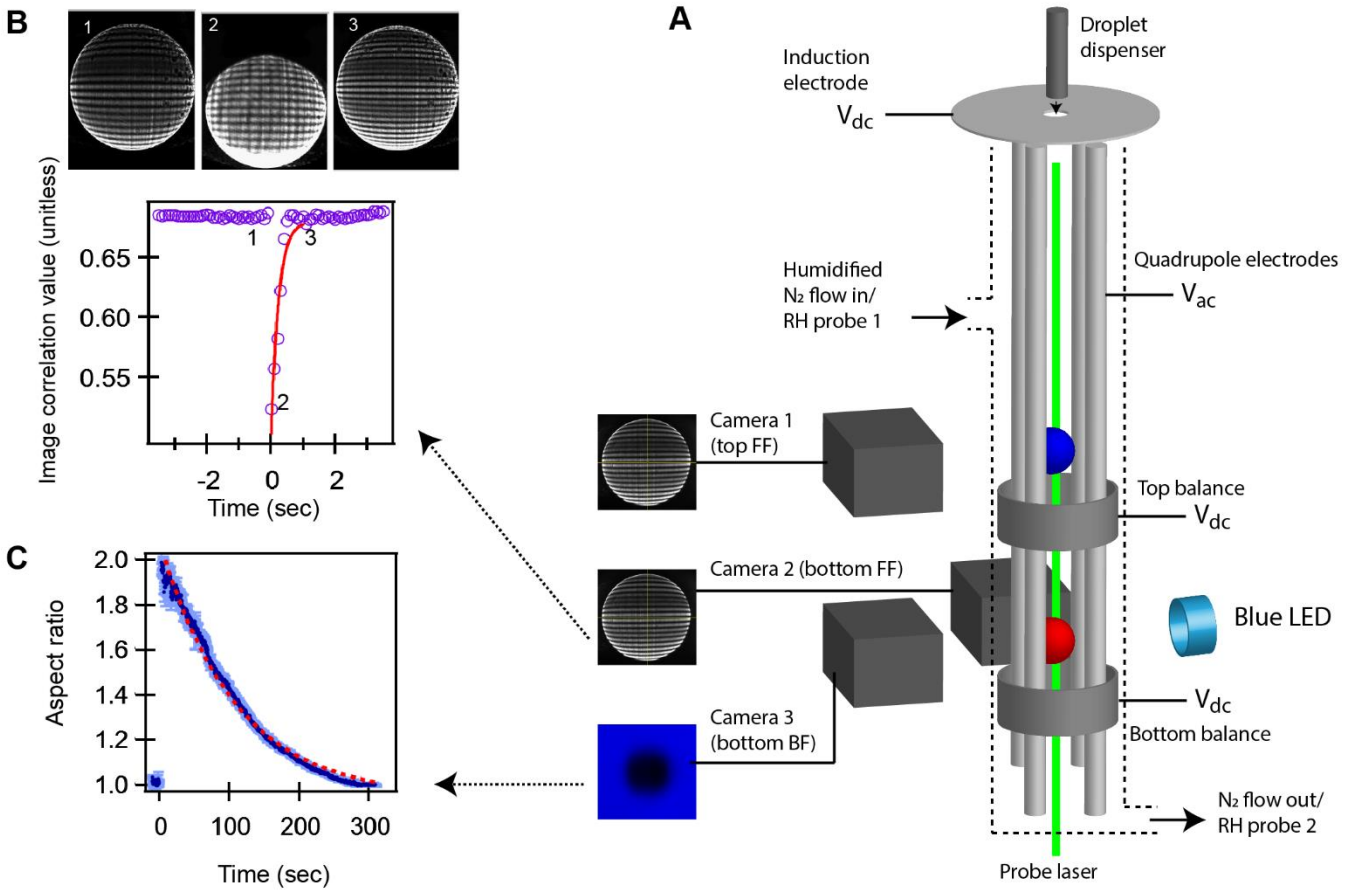

Figure S1. Experimental overview. **(A)** The experimental arrangement of the dual-balance linear quadrupole electrodynamic balance (DBQ-EDB) (*14*). Droplets are injected into the trap through an induction plate with applied DC voltage. The quadrupole electrodes with applied AC field confine the charged droplets axially. Two counterbalances (top and bottom) with applied DC voltage counter the force of gravity as well as the drag force from a downward directed humidified N_2 gas flow. By trapping a droplet in the bottom balance first, and then another in the top balance, two droplets can be levitated simultaneously, one directly above the other. The ambient RH is measured with RH probes placed at the gas flow inlet and outlet. The chamber is housed in quartz tubing. A 532 nm probe laser illuminates the droplets from below. The laser is not necessary for trapping or merging droplets, and is only used to verify initial trapping and for droplet positioning. The laser is turned off when not necessary. The droplet in the top balance is monitored with far-field (FF) imaging (camera 1). The droplet in the bottom balance is monitored with far-field imaging (camera 2) and is also illuminated with a blue LED for bright-field imaging (camera 3). **(B)** Far-field image analysis to determine τ for rapid merging events ($\tau < 3$ sec). Original far-field images (top) for a merging event of ternary Ca-glucose droplets at 41% RH. Panel 1: pre-merging. Panels 2 and 3 show the merging and coalescence process. A plot of correlation value C (Eq. 1) as a function of time is shown beneath the far-field images. Image numbers indicated on the plot correspond to the images shown. An exponential fit (red line) was used to determine the time-constant τ for the merging event ($\tau = 0.23 \pm 0.03$ sec). **(C)** Aspect ratio as a function of time for a merging event of binary gluconic acid after 5 min equilibration time at 10±2% RH ($\tau = 107 \pm 1$ sec), respectively. Each data point represents the average aspect ratio of five sequential images. Shaded portion is ±1 SD. Dashed red line is the exponential fit.

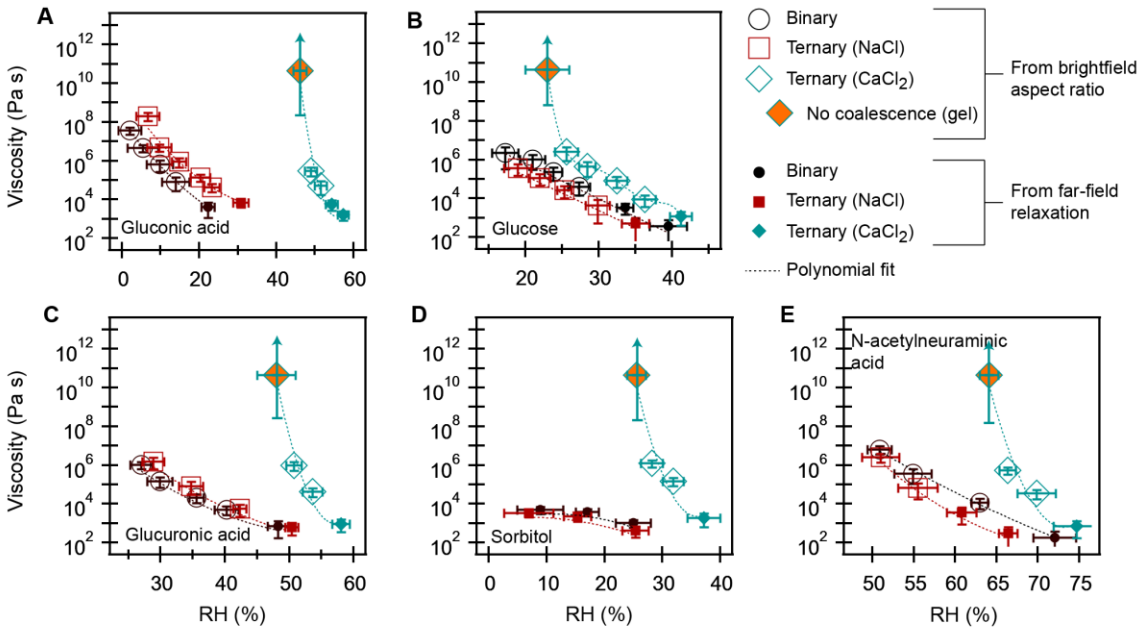

Figure S2. The data shown in Fig. 2A-E of the manuscript, along with ternary NaCl-organic data, converted to estimated viscosity under the experimental conditions (with a droplet equilibration time of 5 min) from Eq. S1 using a surface tension value of 55±30 mN m^{-1} for binary organics and 80±30 mN m^{-1} for ternary mixtures, and a droplet diameter of 36±4 μm. Measured τ values were used where appropriate. For rigid gels, the τ values were estimated from Fig. S3 assuming Newtonian behavior. Note: for instances in which no coalescence was observed (i.e., presumed gel formation) the particles may be non-Newtonian and not fully described with a single dynamic viscosity (*14*), where the estimated viscosity shown here may be representative of the effect of the solid network, but may not be representative of any fluid contained within the pores. Thus, the mechanism of diffusion through the droplet may not be readily inferred from Stokes-Einstein (Eq. S2) alone. However, there is insufficient evidence to suggest Newtonian vs. non-Newtonian dynamics at this time and we have thus attempted to constrain the rigidity of these particles using a τ value of $1x10^7$ sec, with the lower limit to the error bars representing the experimental t_{obs}. The upper limit to viscosity is not known.

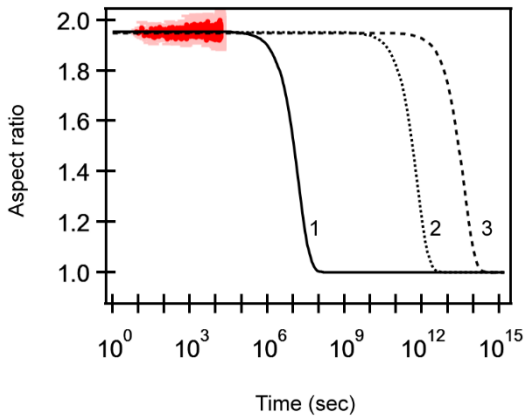

Figure S3. Attempts to extract time constants from aspect ratio as a function of time for merged gels assuming they would ultimately coalesce (although this assumption is not necessarily valid) and with varying fit coefficients. The data was fit to an exponential with the form $f(t) = y_o + A \cdot \exp(-t/\tau)$, where y_o, A and τ are fit parameters. If coalescence were to occur, y_o would be equal to one (the aspect ratio of a sphere). Thus, to estimate τ if coalescence were to occur, y_o was held at a fixed value of 1 for τ estimates. Plots 1 to 3 show the estimated τ as A is varied. In plot 2, both A and τ were allowed to be iteratively varied in the fitting program, with computed fit coefficient outputs of $A = 0.9526 \pm 0.0002$ and $\tau = 7 \times 10^{11} \pm 9 \times 10^{15}$ sec. In plot 1, A was held fixed at $A = 0.955$. In this case, $\tau = 1.7(\pm 0.3) \times 10^{7}$ sec. In plot 3, A was held fixed at $A = 0.950$. In this case, $\tau = 4 \times 10^{13} \pm 2 \times 10^{19}$ sec. The wide variation in τ (from 10^7 to 10^{13} sec) as A is varied demonstrates the large uncertainty with making any determination of τ (if applicable). In Fig. 2F-I and Fig. 3B of the manuscript, and Fig. S2 of the SI, the value of 10^7 sec is used for τ when constraining viscosity.

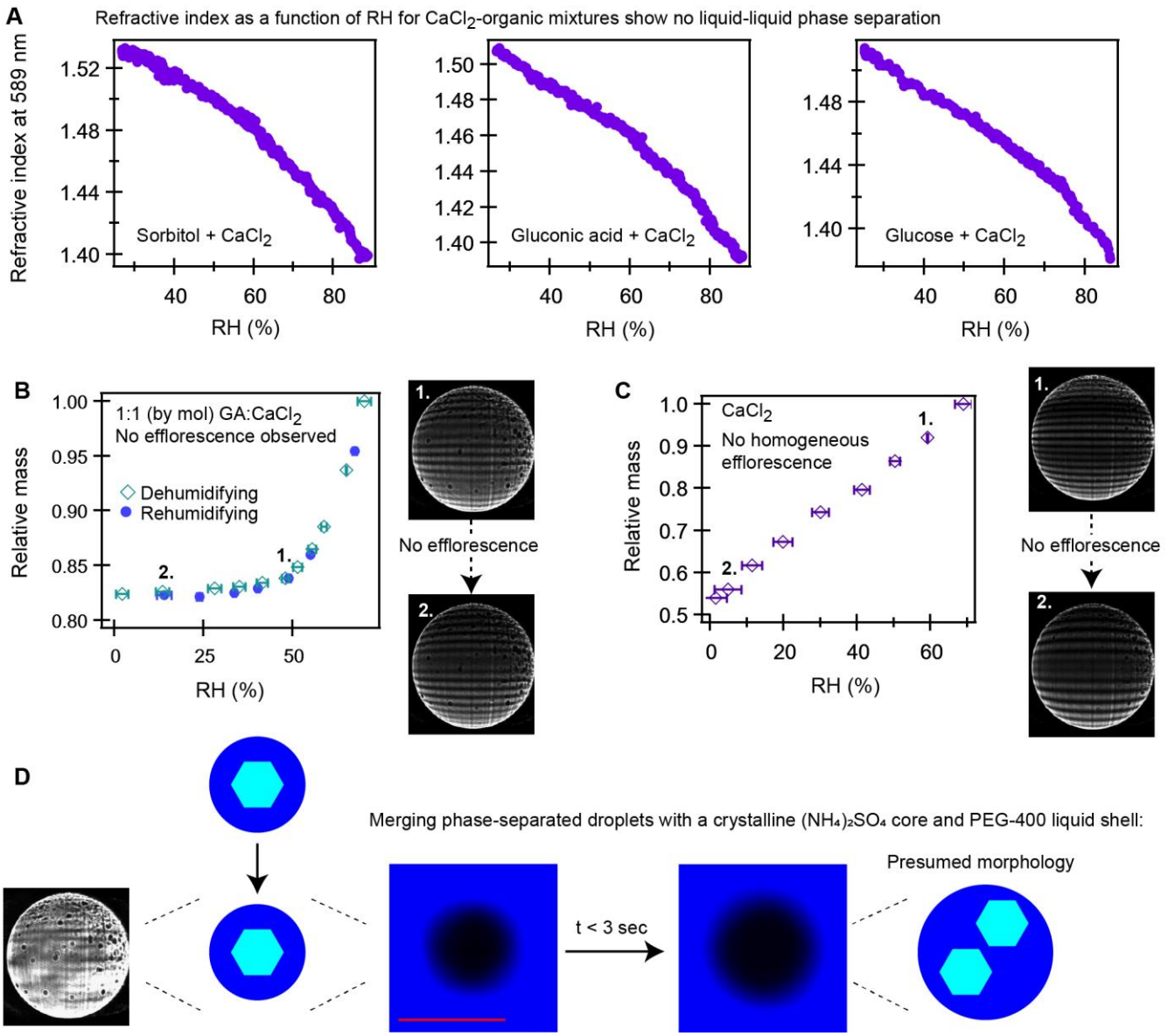

Figure S4. Ruling out liquid-liquid phase separation and efflorescence in the systems studied. **(A)** Refractive index, obtained using Mie resonance spectroscopy of levitated droplets (*35*), as a function of RH for representative $CaCl_2$-organic mixtures show that there is no abrupt discontinuity in refractive index, which is evidence that these mixtures remain as homogeneously-mixed droplets, consistent with our observations that the ternary Ca systems have higher viscosity than the binary systems alone; were the Ca-organic droplets phase separated as liquids, the inferred viscosity would not be higher than the individual components. **(B)** Far-field laser scatter imaging and relative mass measurements of single droplets, shown here for 1:1 gluconic acid (GA): $CaCl_2$, demonstrate that there is no abrupt change in mass that would indicate efflorescence, and there is no evidence for crystallization in the far-field images, as evident by the linear interference fringes that are consistent with a spherical (non-crystalline) droplet (*4,14*). Furthermore, there is no strong hysteresis upon rehumidification, which is typically observed with efflorescence (*5*). Thus, we conclude that there is no efflorescence in the $CaCl_2$-organic mixtures. **(C)** Further, as shown here, $CaCl_2$ does not homogeneously effloresce, which makes it unlikely that it would effloresce even if LLPS were to occur. **(D)** In our setup, if phase-separated droplets partially effloresce (in this instance, 1:1 ammonium sulfate:polyethylene glycol-400 (PEG-400), which phase separates (*10*)), it is readily apparent, as seen in the far-field images (inset, lower left). If partially-effloresced, phase-separated droplets are merged at 30% RH, the droplets rapidly and fully coalesce, indicating the liquid shell is thick enough to encompass the crystalline material (which may exist as multiple small crystals (*10*)). This is in contrast to our observations of Ca-organic droplets, which remained as rigid dimers.

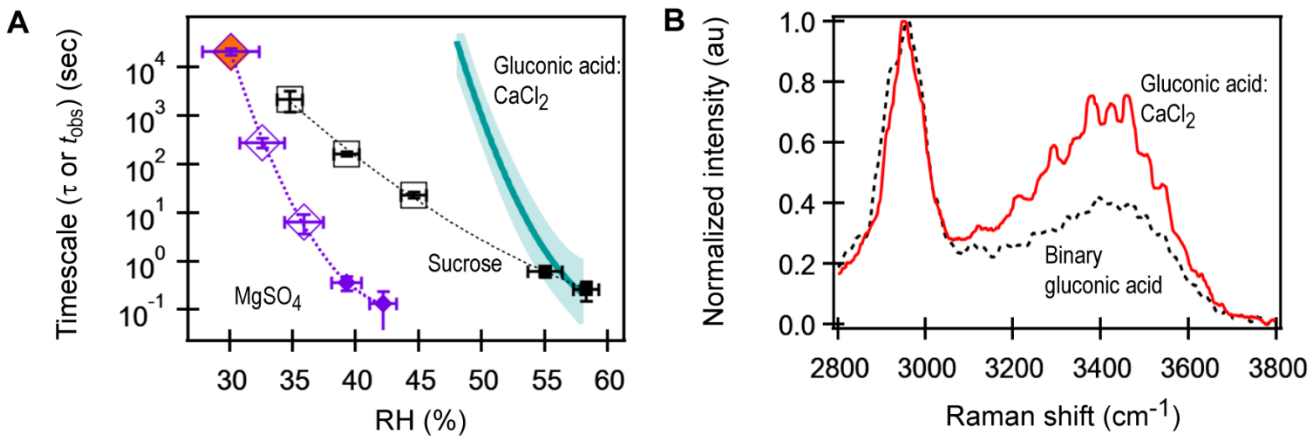

Figure S5. Additional evidence for hydrogel formation. **(A)** Measured values of RH-dependent timescales associated with merging events for binary sucrose (black squares) and binary $MgSO_4$ (purple triangles). Data for $MgSO_4$ and sucrose is adapted from Richards et al. (*14*). If coalescence was observed, average τ (±1 SD) is reported. If no coalescence was observed and merged dimers were rigid, average t_{obs} (±1 SD) is reported. Orange filled triangle indicates gel. Open markers: bright-field. Closed markers: laser scatter. For comparison, the polynomial fit to the data for 1:1 $CaCl_2$:gluconic acid is shown (green line; shaded region represents the 75th percentile confidence band of the fit). **(B)** Raman spectrum of levitated binary gluconic acid droplets (black line) and ternary 1:1 $CaCl_2$:gluconic acid droplets (red line) at 40% RH. Spectra were normalized to the C-H stretch of gluconic acid. (~2900 cm^{-1}). The magnitude of the O-H band (from water) (centered on ~3200-3600 cm^{-1}) for the ternary mixture is nearly double that of the binary organic, demonstrating increased water content in the ternary mixture relative to that of the binary.

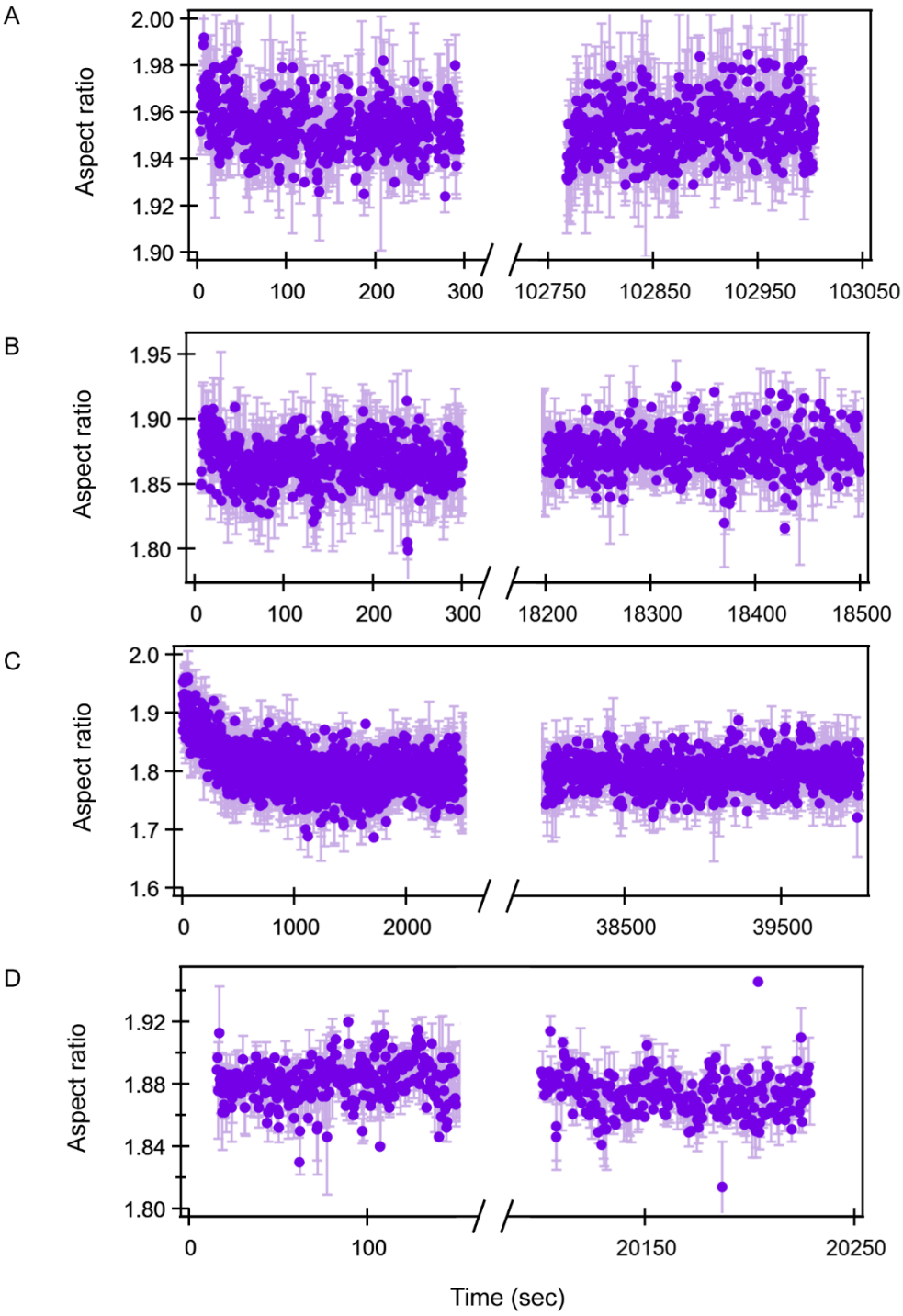

Figure S6. Additional examples of aspect ratio as a function of time for merged, rigid particles of ternary 1:1 $CaCl_2$:organic droplets (presumed gels). **(A)** 1:1 $CaCl_2$:glucose at 22±3% RH, **(B)** 1:1 $CaCl_2$:N-acetylneuraminic acid at 64±2% RH, **(C)** 1:1 $CaCl_2$:glucuronic acid at 47±2% RH (with an initial decay in aspect ratio from 2 to ~1.8 followed by rigidity (no further coalescence) suggestive of non-Newtonian dynamics (*14*)), and **(D)** 1:1 $CaCl_2$:sorbitol at 25±3% RH. Each data point is the average aspect ratio of five sequential images (±1 SD).

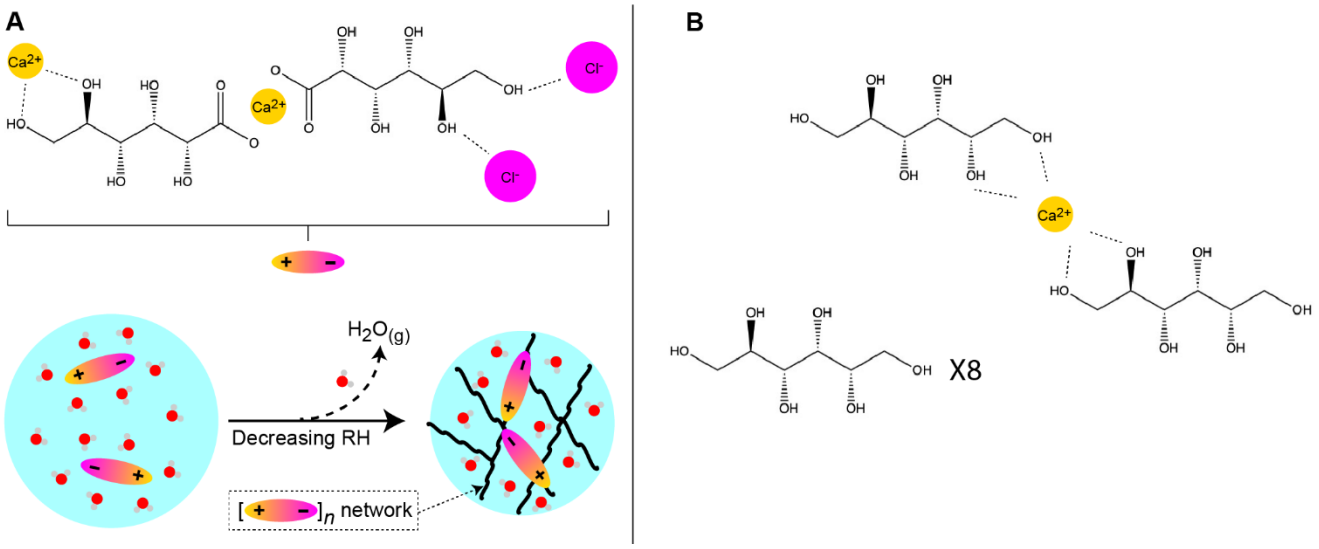

Figure S7. Proposed supramolecular effects between divalent ions and oxygenated organics. (**A)** One proposed pathway for assembly of gels from Ca^{2+}, Cl^- and carboxylated organics, such as gluconic acid, with gluconate chelating Ca^{2+}, effectively forming a larger saccharide. Ion-organic complexes then assemble through long-range ion-paired networks upon decreasing water content. **(B)** Proposed short-range Ca-sorbitol units in 10:1 sorbitol:$CaCl_2$ mixtures. Shown here is two sorbitol molecules forming supramolecular linkages with one Ca^{2+}, with eight unbound sorbitol molecules. The effective molecular weight of the mixture increases, potentially leading to increased viscosity.

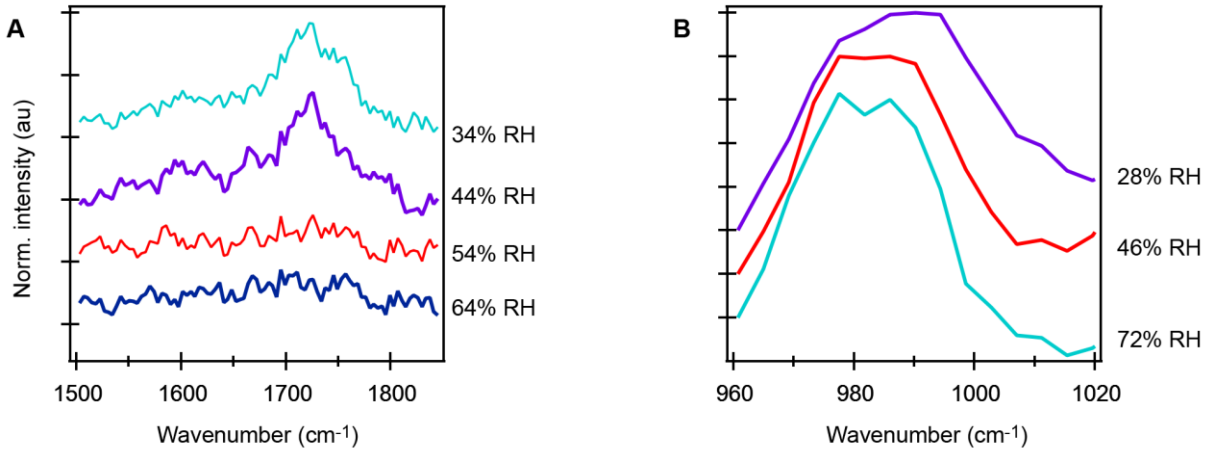

Figure S8. Raman spectra showing evidence for ion-pairing. **(A)** Raman spectra of a 1:1 $CaCl_2$-gluconic acid droplet focusing on the spectral region associated with the carboxylate group (*40*). Below the gel transition RH of this system (~46% RH) there is an increase in intensity and changes within the carboxylate region, potentially due to changes in the degree of hydration of Ca binding to the carboxylate group (*40*). This suggests the cation is interacting with the organics more strongly at the gel transition RH and below. With Cl- as the anion, we cannot observe any changes in the Raman structure because Cl is not Raman active. **(B)** To monitor changes associated with anions, we used 1:1 $MgSO_4$-gluconic acid and focused on the SO_4 spectral region. As shown here, the sulfate peak shifts to higher wavenumbers and broadens below the gel transition RH (~32% RH). These shifts have previously been shown to be associated with contact ion pairing in aqueous $MgSO_4$ solutions (*24*). Thus, in part A, there is evidence for ion binding with the organic (gluconic acid), in part B there is evidence for the anion forming contact ion pairs. Combined, these spectral changes suggest the gel transition is the result of synergistic, organic-mediated ion-pairing that form long-range supramolecular networks.

Table S1. AIOMFAC[a] predicted water content of binary and ternary $CaCl_2$:gluconic acid droplets at 40% RH[b]

Composition	Mass fraction $CaCl_{2(aq)}$	Mass fraction gluconic acid (aq)	**Mass fraction H_2O**
Binary	--	0.86	**0.14**
Ternary	0.26	0.47	**0.27**

[a]AIOMFAC model (ref 29): https://aiomfac.lab.mcgill.ca/model.html

[b]The RH at which Raman spectra were collected for comparison of the binary and ternary mixtures. The spectra are shown in Fig. S5B.